Kinetics and Mechanism of Transamination Reaction of L-Phenylalanine with Hydrophobic Pyridoxal in Vesicular and Micellar Phases

Yukito Murakami,* Jun-ichi Kikuchi, Kazunari Akiyoshi, and Toru Imori
Department of Organic Synthesis, Faculty of Engineering, Kyushu University, Fukuoka 812, Japan

A hydrophobic pyridoxal derivative quaternized at the pyridyl nitrogen with a double-chain segment (PL^+2C_{16}) was embedded in the single-walled vesicle of *NN*-dihexadecyl-N^{α}-[6-(trimethylammonio)hexanoyl]-L-alaninamide bromide ($N^+C_5Ala2C_{16}$), and the pyridoxal moiety was fixed in the hydrogen-belt domain of the vesicle. While the transamination of L-phenylalanine (L-Phe), a hydrophobic α-amino acid, with PL^+2C_{16} in the vesicle and the hexadecyltrimethylammonium bromide (CTAB) micelle proceeded slowly to afford the pyridoxamine derivative (PM^+2C_{16}) and β-phenylpyruvic acid, addition of metal ions to the equilibrium mixture of the aldimine Schiff's base (ASB), PL^+2C_{16}, and L-Phe caused acceleration of the overall transamination rate. The transamination was most effectively catalysed by copper(II) ions in the $N^+C_5Ala2C_{16}$ vesicle and the CTAB micelle. The catalytic activity of copper(II) ions was so enhanced as to allow significant accumulation of the carbanion chelate, derived from the ASB chelate by α-hydrogen removal, as an intermediate in the aldimine–ketimine isomerization. The reactivity of the overall copper(II)-catalysed transamination was greater in the vesicle than in the micelle and primarily controlled by the collapse ratio of the copper(II)–carbanion species as clarified by detailed kinetic analysis.

The biological transamination of an α-amino acid with an α-keto acid, catalysed by the vitamin B_6-dependent transaminase, proceeds through a shuttle mechanism involving reversible isomerization between two pairs of aldimine Schiff's bases and the corresponding ketimine Schiff's bases.[1] Even though the role of the coenzyme, pyridoxal 5′-phosphate, has been clarified by adopting simple model systems, the catalytic activity of such systems has been far less efficient than that of the enzyme.[1,2] We have been dealing with functionalized bilayer co-vesicles, each composed of a synthetic peptide lipid and a hydrophobic vitamin B_6 analogue, as artificial transaminases. Such holoenzyme model systems have the following characteristic features. (i) Bilayer vesicles composed of synthetic peptide lipids are morphologically extremely stable[3] and can be used as steady hydrophobic media for transamination. (ii) The pyridoxal or the pyridoxamine moiety, which is modified with a hydrophobic segment, is readily placed in the hydrogen-belt domain interposed between the polar surface region and the hydrophobic domain composed of double-chain segments within the bilayer assembly.[4] (iii) Formation of a Schiff's base, which is derived from a vitamin B_6 analogue and an α-amino acid or an α-keto acid as a reaction intermediate, is much enhanced in the quasi-hydrophobic hydrogen-belt domain.[5] (iv) Since Schiff's base formation takes place in the quasi-hydrophobic intramembrane domain, substrate selectivity for the incorporation of α-amino acids and α-keto acids controls the extent of the reaction.[6] (v) When catalytically active amino acid residues involved in synthetic peptide lipids are placed in the hydrogen-belt domain, they exercise co-operative catalysis with the coenzyme moiety.[4–6]

In contrast with extensive studies on the transamination of pyridoxamine derivatives with α-keto acids in the presence and absence of metal ions,[7–11] detailed studies on the kinetics and mechanism of the reverse reaction, the transamination of α-amino acids with pyridoxal derivatives, have been carried out only to a limited extent.[7b,c,12,13] As reported in our preliminary communication, a hydrophobic α-amino acid readily undergoes transamination with a hydrophobic pyridoxal derivative quaternized at the pyridyl nitrogen, 1-(*NN*-dihexadecylcarbamoylmethyl)-2-methyl-3-hydroxy-4-formyl-5-hydroxymethylpyridinium chloride (PL^+2C_{16}), in single-walled bilayer vesicles.[6a] Addition of copper(II) ions to the reaction system resulted in marked acceleration of the rate, and general acid–base catalysis by the imidazolyl group further promoted the reaction when *NN*-dihexadecyl-N^{α}-[6-(trimethylammonio)hexanoyl]-L-histidinamide bromide ($N^+C_5His2C_{16}$) was used as a bilayer-forming lipid. In this work, we investigated the kinetics and mechanism of the transamination of L-phenylalanine with PL^+2C_{16} in the single-walled vesicle of *NN*-dihexadecyl-N^{α}-[6-(trimethylammonio)hexanoyl]-L-alaninamide bromide ($N^+C_5Ala2C_{16}$) and the micelle of hexadecyltrimethylammonium bromide (CTAB). The $N^+C_5His2C_{16}$ vesicle is far more effective than the molecular aggregates of $N^+C_5Ala2C_{16}$ and CTAB for acceleration of the present transamination as mentioned above.[6a] However, critical analysis of kinetic data was not possible since the aldimine Schiff's base did not form quantitatively in the initial stage of the reaction carried out in the $N^+C_5His2C_{16}$ vesicle.

Results and Discussion

Microenvironments around the Pyridoxal Moiety in Molecular Aggregates.—The sonicated lipid system composed of $N^+C_5Ala2C_{16}$ and PL^+2C_{16} (molar ratio, 20:1) forms single-walled co-vesicles, which are intrinsically identical with single-walled vesicles of $N^+C_5Ala2C_{16}$ without any co-existing component[3] (Figure 1). The phase transition temperature for the present single-walled co-vesicle was evaluated from the temperature-dependent steady-state fluorescence anisotropy (r_s) of 1,6-diphenylhexa-1,3,5-triene (DPH) which is embedded in the hydrophobic domain of the aggregate. As shown in Figure 2A, the phase transition from gel to liquid crystalline state takes place over a wide temperature range, 20 ± 5 °C. This value is identical with that observed for the single-walled vesicle of $N^+C_5Ala2C_{16}$ alone by fluorescence polarization spectroscopy[4b] and differential scanning calorimetry.[3] On the other hand, the r_s value for the aggregate composed of CTAB and PL^+2C_{16} (molar ratio, 60:1) changes regularly without showing any inflection range over the same temperature region and is lower than that for the vesicular system at each

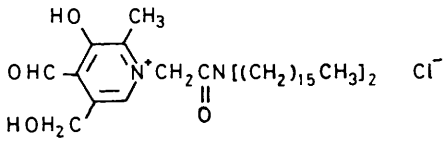

$PL^{+}2C_{16}$

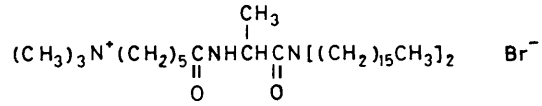

$N^{+}C_5Ala2C_{16}$

temperature (Figure 2A). The latter behaviour reflects that the hydrophobic domain of the CTAB micellar system is more disordered than that of the $N^{+}C_5Ala2C_{16}$ vesicular system.

The parameters for steady-state fluorescence anisotropy originated from the pyridoxal moiety of $PL^{+}2C_{16}$ embedded in both micellar and vesicular systems do not show any inflection temperature ranges as shown in Figure 2B. This indicates that the pyridoxal moiety is fixed in the hydrogen-belt domain of the vesicle, where its molecular motion is little affected by the phase transition occurring in the hydrophobic domain. The microenvironmental polarities around the pyridoxal moiety of $PL^{+}2C_{16}$ incorporated into the molecular aggregates were evaluated by spectrophotometric means in the light of our observation that the electronic absorption maximum ($\lambda_{max.}$) for $PL^{+}2C_{16}$ with the deprotonated 3-hydroxy group undergoes a red shift with decrease in medium polarity. The pyridoxal moiety is placed in the microenvironments equivalent to those provided by propan-1-ol [E_T(30) 50.7] and methanol [E_T(30) 55.5] in the $N^{+}C_5Ala2C_{16}$ vesicle ($\lambda_{max.}$ 338 nm) and the CTAB micelle ($\lambda_{max.}$ 335 nm), respectively. Since the r_s value for non-aggregated $PL^{+}2C_{16}$ increased as the medium polarity increased in homogeneous aqueous solutions containing dioxane in the 60—95% (v/v) range, the fluorescence lifetime of the pyridoxal moiety must decrease as the microenvironmental polarity around it is raised. This effect seems to explain the reason why the r_s value is greater in the CTAB micelle relative to that in the $N^{+}C_5Ala2C_{16}$ vesicle (Figure 2B).

Transamination of L-*Phenylalanine with* $PL^{+}2C_{16}$ *in Molecular Aggregates.*—The pH-dependent equilibrium constant (K_{SB}), as defined by equation (1), for the aldimine Schiff's base (ASB) formation between $PL^{+}2C_{16}$ and an α-amino acid (AA) was evaluated as follows. Various amounts of AA (5.0 ×

$$K_{SB} = [ASB]/([PL^{+}2C_{16}][AA]) \quad (1)$$

10^{-4}—5.0 × 10^{-2} mol dm^{-3}) were added to the aqueous carbonate buffer containing $PL^{+}2C_{16}$ (5.0 × 10^{-5} mol dm^{-3}), and electronic absorption spectra were recorded after the equilibrium was attained within 30 min. The K_{SB} value was calculated on the basis of the Benesi–Hildebrand relationship {equation (2)[14] where ΔA is the absorbance change upon

$$1/\Delta A = 1/(\Delta\varepsilon[PL^{+}2C_{16}]_0) + 1/(\Delta\varepsilon K_{SB}[PL^{+}2C_{16}]_0[AA]_0) \quad (2)$$

addition of AA at the absorption maximum of ASB, $\Delta\varepsilon$ stands for the difference in molar absorption coefficient between ASB and $PL^{+}2C_{16}$, and $[PL^{+}2C_{16}]_0$ and $[AA]_0$ are the initial

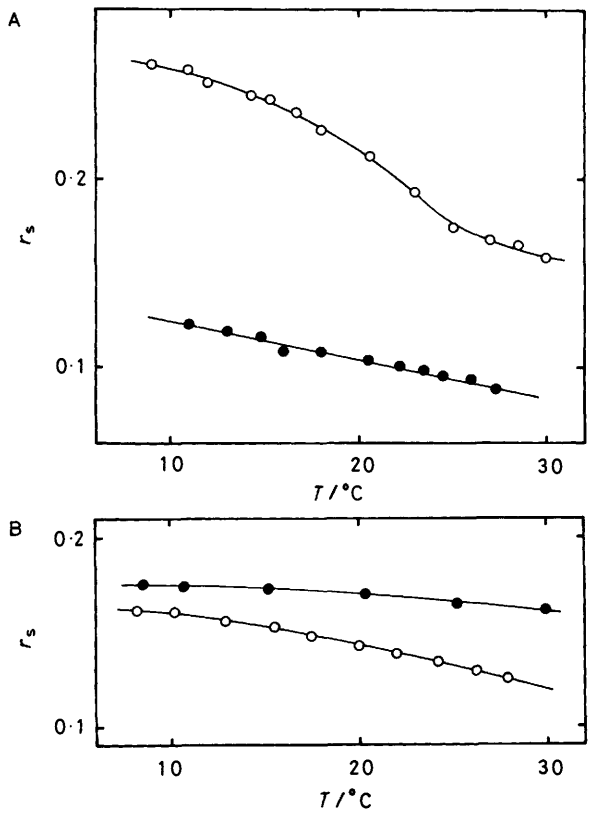

Figure 2. Correlations of temperature with steady-state fluorescence anisotropy (r_s) for probes embedded in the $N^{+}C_5Ala2C_{16}$ (1.0 × 10^{-3} mol dm^{-3}) single-walled vesicle (○) and the CTAB (3.0 × 10^{-3} mol dm^{-3}) micelle (●), both containing $PL^{+}2C_{16}$ (5.0 × 10^{-5} mol dm^{-3}) in an aqueous carbonate buffer (2.0 × 10^{-2} mol dm^{-3}) at pH 9.9 and μ 0.10 (KCl): A, r_s originated from DPH (1.0 × 10^{-7} mol dm^{-3}); B, r_s originated from the pyridoxal moiety of $PL^{+}2C_{16}$ in the absence of DPH. Excitation and emission wavelengths are 340 and 450 for DPH and 340 and 400 nm for $PL^{+}2C_{16}$, respectively

concentrations of $PL^{+}2C_{16}$ and AA, respectively}. The K_{SB} values with various α-amino acids in the $N^{+}C_5Ala2C_{16}$ vesicle and in the CTAB micelle are listed in Table 1.

The extent of formation of the aldimine Schiff's base (ASB in Scheme 1) of $PL^{+}2C_{16}$ with an α-amino acid in the $N^{+}C_5Ala2C_{16}$ vesicle and the CTAB micelle is dependent on the hydrophobicity of an α-amino acid. The pH-dependent equilibrium constants for $PL^{+}2C_{16}$ with a hydrophobic α-amino acid used here, L-phenylalanine (L-Phe), are 1 700 and 2 100 dm^3 mol^{-1} in the vesicle and the micelle, respectively, and much larger than the value obtained for 1,2-dimethyl-3-hydroxy-4-formyl-5-hydroxymethylpyridinium chloride ($PL^{+}C_1$) with L-Phe in the aqueous carbonate buffer (K_{SB} 10 dm^3 mol^{-1}). Because of the more favourable formation of the aldimine Schiff's base with L-Phe, this α-amino acid was used exclusively for the present kinetic investigation. In the absence of metal ions, the transamination reaction in each molecular aggregate system proceeded slowly to give the pyridoxamine derivative ($PM^{+}2C_{16}$) and β-phenylpyruvate (KA); the apparent first-order rate constants (k_{obs}), evaluated from the disappearance of ASB ($\lambda_{max.}$ 393 nm) and the appearance of $PM^{+}2C_{16}$ ($\lambda_{max.}$ 335 nm), are 1.5 × 10^{-6} and 2.1 × 10^{-6} s^{-1} in the vesicular and micellar systems, respectively, at 30.0 °C with the following initial concentrations (in mol dm^{-3}) and medium conditions: $PL^{+}2C_{16}$, 5.0 × 10^{-5}; L-Phe, 5.0 × 10^{-3}; $N^{+}C_5Ala2C_{16}$, 1.0 × 10^{-3}; CTAB, 3.0 × 10^{-3}; ethylenediaminetetra-acetate, 1.0 × 10^{-4}; medium, an aqueous carbonate buffer (0.02 mol

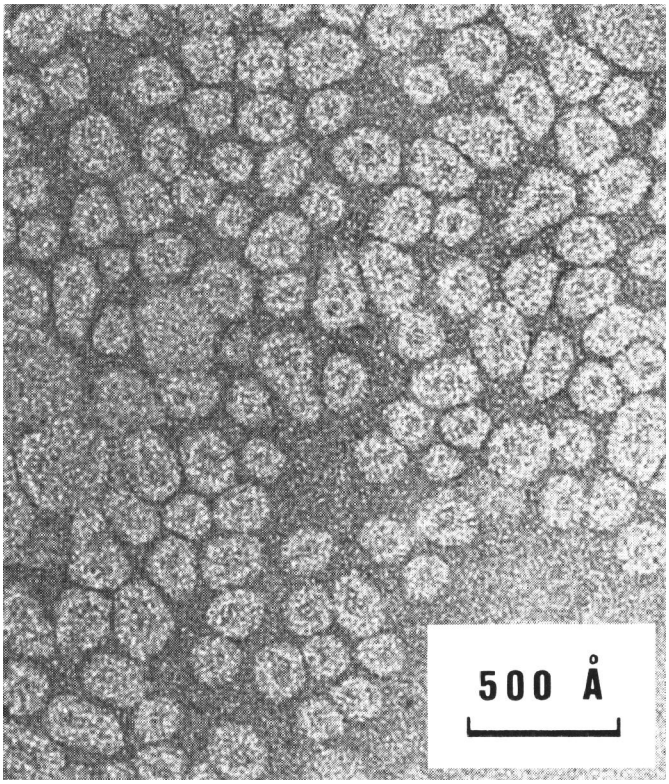

Figure 1. Negatively stained electron micrograph for co-vesicles composed of $N^+C_5Ala2C_{16}$ (1.0×10^{-3} mol dm^{-3}) and PL^+2C_{16} (5.0×10^{-5} mol dm^{-3}); sonicated for 1 min at 30 W

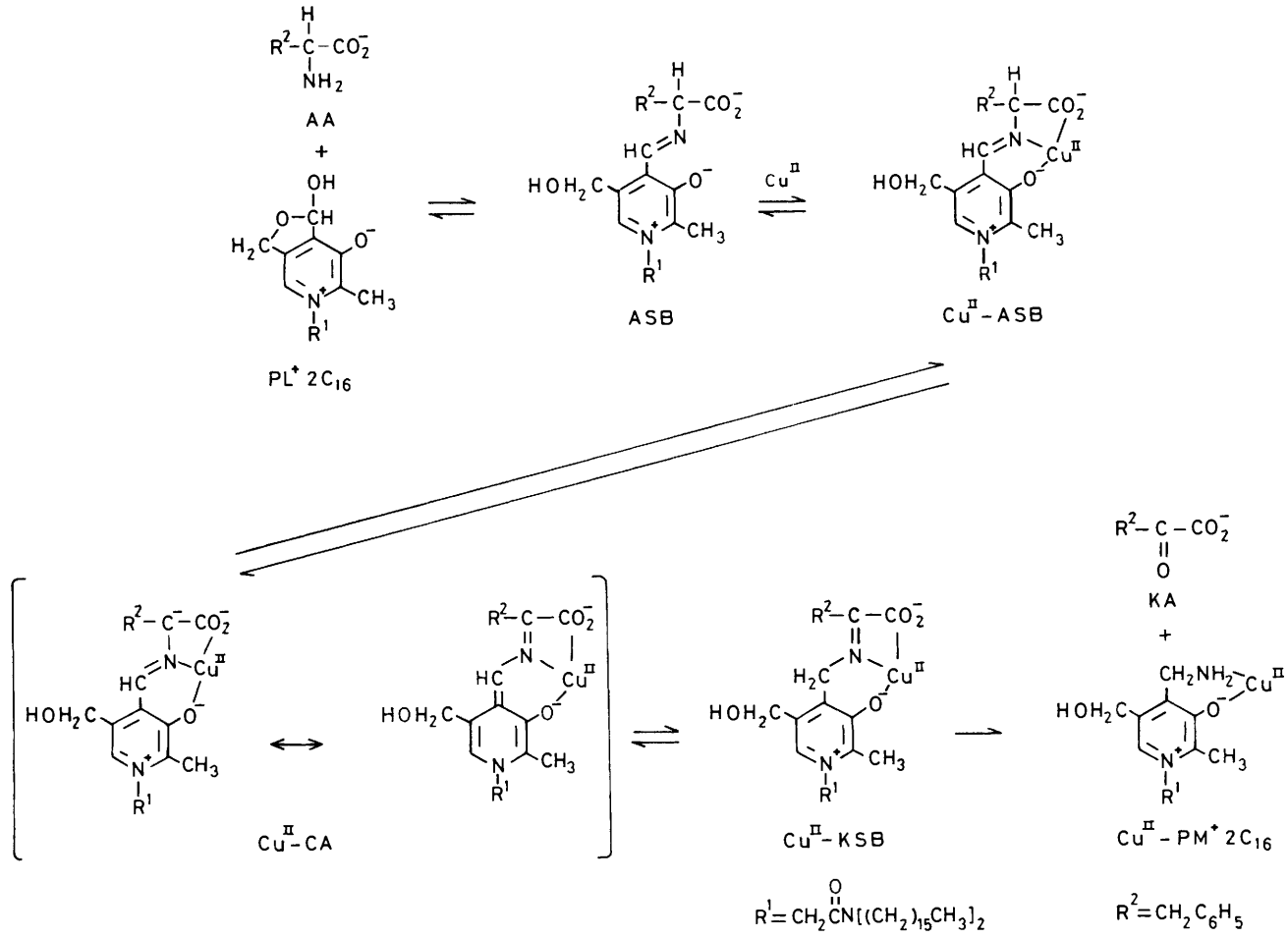

Scheme 1.

dm^{-3}) at pH 9.9 and μ 0.10 (KCl). Because of the large K_{SB} values and the rapid attainment of the equilibrium in both molecular aggregates, the rate constants (k) for isomerization, defined in equation (3), are nearly equivalent to the k_{obs} values under the present conditions: k values are 1.6×10^{-6} and 2.1×10^{-6} s^{-1} at 30.0 °C in the vesicle and the micelle, respectively.

$$PL^{+}2C_{16} + \text{L-Phe} \overset{K_{SB}}{\rightleftharpoons} ASB \xrightarrow{k} PM^{+}2C_{16} + KA \quad (3)$$

Since accumulation of the intermediate ketimine Schiff's base (KSB) was not detected at all by spectroscopic means in both aggregates, the isomerization from ASB to KSB must be the rate-determining step in the overall reaction.

Addition of metal ions to the equilibrium mixture of ASB, $PL^{+}2C_{16}$, and L-Phe, which was obtained in the fast initial step, caused acceleration of the overall transamination reaction. As listed in Table 2, the catalytic activity of copper(II) ions is by far the highest among those of various metal ions employed here. The copper(II) complex of the carbanion intermediate (Cu^{II}-CA in Scheme 1; $\lambda_{max.}$ 523 nm), derived from Cu^{II}-ASB by α-hydrogen removal, was observed spectrophotometrically during the reaction in each molecular aggregate as typically shown for the micellar system (Figure 3). On the other hand, the corresponding metal–carbanion chelates were not detected in the other metal-catalysed systems. The result strongly indicates that square-planar co-ordination geometry around the metal ion is important for effective electron delocalization throughout the Cu^{II}-ASB and Cu^{II}-CA molecules as well as for labilization of the α-hydrogen atom of ASB. Both effects act to promote isomerization.

Several studies have been carried out on the carbanion species absorbing in the 500 nm range. These were derived from combinations of pyridoxal derivatives and α-amino acids in the active site of aspartate aminotransferase.[15] As for non-enzymatic reactions, carbanion species were derived from the corresponding aldimine Schiff's bases formed with pyridoxal analogues and α-amino acid esters in methanol; the aldimine Schiff's bases were activated by quaternization of the pyridyl nitrogen[16] on one hand and by co-ordination of tervalent metal ions on the other.[17] Extremely poor yields of the carbanion species were also observed during the transamination reaction of 1-methyl-4-formylpyridinium iodide with glycine and alanine in aqueous media.[13a] Since they failed to evaluate the formation of those carbanion species quantitatively, detailed kinetic analyses were not carried out for those enzymatic and non-enzymatic systems.

Addition of 5,5′-dithiobis-(2-nitrobenzoic acid) (DTNB), which is an effective reagent for reaction with carbanions, to the copper(II) chelate system in both micellar and vesicular phases at pH 10.6 and 6.0 °C resulted in instantaneous appearance of a new absorption band in the 420 nm range, a characteristic band for 3-carboxy-4-nitrothiophenolate anion, with concomitant disappearance of the carbanion species. For evaluation of amounts of the copper(II)–carbanion chelate, the absorbance

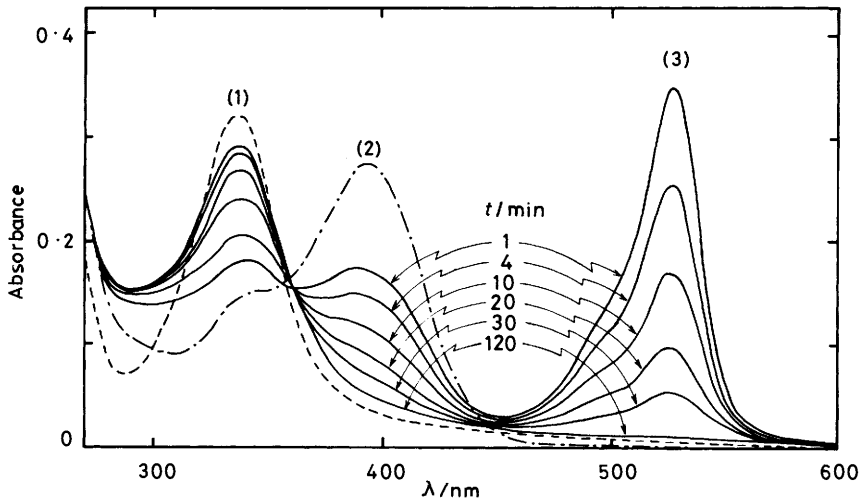

Figure 3. Absorption spectral changes for the Cu^{II}-catalysed transamination of L-Phe (5.0×10^{-3} mol dm^{-3}) with $PL^{+}2C_{16}$ (5.0×10^{-5} mol dm^{-3}) in the presence of CTAB (3.0×10^{-3} mol dm^{-3}) in an aqueous carbonate buffer (2.0×10^{-2} mol dm^{-3}, pH 9.9, μ 0.10 with KCl) at 30.0 °C: (1) (– – –), $PL^{+}2C_{16}$ alone; (2) (— · — · —), equilibrium mixture of $PL^{+}2C_{16}$, L-Phe, and ASB (Scheme 1) without Cu^{II}; (3) (——), Cu^{II} complex species formed upon addition of $Cu(ClO_4)_2$ (5.0×10^{-5} mol dm^{-3}) to (2). The curves in (3) are distinguished by figures which give the reaction period (t) in min after addition of copper(II) ions

Table 1. pH-Dependent equilibrium constants (K_{SB}/dm^3 mol^{-1}) for formation of aldimine Schiff's bases derived from $PL^{+}2C_{16}$ and α-amino acids in molecular aggregates at 30.0 °C[a]

Amino acid	$N^{+}C_5Ala2C_{16}$ vesicle	CTAB micelle
L-Phenylalanine	1 700[b]	2 100
L-Isoleucine	900	1 100
L-Leucine	560[b]	790
L-Valine	270	370
L-Alanine	10[b]	10
L-Glutamic acid		390

[a] In an aqueous carbonate buffer (0.02 mol dm^{-3}) at pH 9.9 and μ 0.10 (KCl). Initial concentrations in mol dm^{-3}: $PL^{+}2C_{16}$, 5.0×10^{-5}; α-amino acids, 5.0×10^{-4}—5.0×10^{-2}; EDTA, 1.0×10^{-4}; $N^{+}C_5Ala2C_{16}$, 1.0×10^{-3}; CTAB, 3.0×10^{-3}. [b] Ref. 6*a*.

Table 2. Metal-ion effects on transamination of L-Phe with $PL^{+}2C_{16}$ in the $N^{+}C_5Ala2C_{16}$ vesicle at 30.0 °C[a]

	Metal ions				
	Cu^{II}	Zn^{II}	Fe^{III}	Al^{III}	None[b]
10^6 k_{obs}/s^{-1}	9 000	37	55	37	1.5

[a] In an aqueous carbonate buffer (0.02 mol dm^{-3}) at pH 9.9 and μ 0.10 (KCl). Initial concentrations in mol dm^{-3}: $PL^{+}2C_{16}$, 5.0×10^{-5}; L-Phe, 5.0×10^{-3}; metal ions, 5.0×10^{-5}; $N^{+}C_5Ala2C_{16}$, 1.0×10^{-3}. [b] EDTA (1.0×10^{-4} mol dm^{-3}) was added.

changes were corrected for spontaneous decomposition of DTNB caused by reaction with hydroxide ions.[18] The identical value was obtained in both micellar and vesicular phases as the molar absorption coefficient of the copper(II)–carbanion chelate; 5.0×10^4 at 523 nm. The maximal concentration of the copper(II)–carbanion chelate formed during the reaction is relatively larger in the CTAB micelle than in the $N^{+}C_5Ala2C_{16}$ vesicle under comparable conditions. However, the transamination reactivity (k_{obs}), as evaluated from the appearance of Cu^{II}-$PM^{+}2C_{16}$ ($\lambda_{max.}$ 335 nm), is higher in the latter than in the former (Table 3).

When 2-methyl-3-hydroxy-4-formyl-5-(dodecylthiomethyl)-pyridine was used in place of $PL^{+}2C_{16}$, the reactivity of

Table 3. Kinetic parameters for isomerization reaction at 15.0 °C[a]

Molecular aggregate	10^2k_1/s^{-1}	10^2k_2/s^{-1}	10^2k_3/s^{-1}	10^3k_{obs}/s^{-1} [b]
$N^{+}C_5Ala2C_{16}$ vesicle	1.3	9.8	1.9	3.4
CTAB micelle	1.8	5.7	0.50	1.1

[a] In an aqueous carbonate buffer (0.02 mol dm^{-3}) at pH 10.6 and μ 0.10 (KCl). Initial concentrations in mol dm^{-3}: $PL^{+}2C_{16}$, 4.5×10^{-5}; L-Phe, 4.5×10^{-3}; $Cu(ClO_4)_2$, 9.0×10^{-5}; $N^{+}C_5Ala2C_{16}$, 1.0×10^{-3}; CTAB, 3.0×10^{-3}. [b] Apparent pseudo-first-order rate constants were evaluated with attention to the formation of Cu^{II}-$PM^{+}2C_{16}$.

transamination with L-Phe was extremely low in the presence and absence of copper(II) ions: the (k_{obs}) values are $< 10^{-6}$ and 6×10^{-5} s^{-1} for metal-free and copper(II)-catalysed systems, respectively, in the $N^{+}C_5Ala2C_{16}$ vesicle under the conditions given in Table 2. In addition, the carbanion species was not detected at all during the reaction. Thus, quaternization of the pyridyl nitrogen makes effective contribution to a change in the rate-determining step and consequently to acceleration of the isomerization.

Kinetic Analysis of Isomerization Process.—The kinetic analysis of the copper(II)-catalysed isomerization was performed under the following conditions. (i) $PL^{+}2C_{16}$ is converted into ASB nearly quantitatively or completely as confirmed by electronic absorption spectroscopy. (ii) The formation of Cu^{II}-ASB from ASB and copper(II) ions is rapid enough to be separated kinetically from the rate-determining isomerization step, *e.g.*, the half-life for the complexation in the CTAB micelle is 0.2 s as evaluated by stopped-flow spectroscopy with attention to an increase in absorbance at 390 nm. (iii) The stability constants for the co-ordination of copper(II) ions to the Schiff's base are sufficiently large in the micellar and vesicular systems,[4a] so that Cu^{II}-ASB is quantitatively formed. (iv) The hydrolysis of Cu^{II}-KSB, which affords Cu^{II}-$PM^{+}2C_{16}$ and KA, is not involved in the rate-determining step as confirmed by spectrophotometric and kinetic means. (v) Copper(II)–Schiff's base complexes are present exclusively as the 1:1 chelates; the copper(II) concentration is in a two-fold molar excess over the concentration of $PL^{+}2C_{16}$.[4a,c] (vi) The outer vesicular layer is exclusively used for isomerization in the $N^{+}C_5Ala2C_{16}$ vesicle,

since the reaction temperature is maintained below T_m of the vesicle. In the light of our previous findings, the permeation of hydrophilic species through single-walled vesicles and the flip-flop behaviour of amphiphile molecules within the vesicular domain do not take place below T_m in a time scale of the isomerization reaction.[3]

The kinetic data for the isomerization were obtained with attention to the absorbance change at 523 nm and analysed by employing a kinetic formula [equation (5)][19] derived on the basis of equation (4). Here, $\lambda_1 = (p + q)/2$, $\lambda_2 = (p - q)/2$,

$$Cu^{II}\text{-ASB} \underset{k_2}{\overset{k_1}{\rightleftharpoons}} Cu^{II}\text{-CA} \xrightarrow{k_3} Cu^{II}\text{-PM}^{+}2C_{16} + KA \quad (4)$$

$$[Cu^{II}\text{-CA}] = \{k_1[Cu^{II}\text{-ASB}]_0/(\lambda_2 - \lambda_1)\} \times \{\exp(-\lambda_1 t) - \exp(-\lambda_2 t)\} \quad (5)$$

$p = k_1 + k_2 + k_3$, and $q = (p^2 - 4k_1k_3)^{\frac{1}{2}}$; $[Cu^{II}\text{-ASB}]_0$ is the initial concentration of Cu^{II}-ASB. As for the CTAB micellar system, $[Cu^{II}\text{-ASB}]_0$ is equal to the initial concentration of $PL^{+}2C_{16}$, $[PL^{+}2C_{16}]_0$. As for the $N^{+}C_5Ala2C_{16}$ vesicular system, however, 74% of the lipid molecules is distributed in the outer layer of the single-walled vesicle as evaluated previously,[3] and the $PL^{+}2C_{16}$ molecules must be homogeneously mixed with the matrix lipid molecules in the membrane since there is no indication of the phase separation: $[Cu^{II}\text{-ASB}]_0 = 0.74[PL^{+}\text{-}2C_{16}]_0$. The absorbance at 523 nm, A_{calc}, was calculated as the product of $[Cu^{II}\text{-CA}]$ [refer to equation (5)] and the molar absorption coefficient of the carbanion complex (ε 5.0×10^4). Thus, the values of k_1, k_2, and k_3 were determined by the regression analysis which minimizes the sum of squares of errors [U; equation (6)], where A_{obs} represents the observed absorbance (Table 3).*

$$U = \sum_t (A_{calc} - A_{obs})^2 \quad (6)$$

Distributions of the three species, Cu^{II}-ASB, Cu^{II}-CA, and $Cu^{II}\text{-PM}^{+}2C_{16}$, which appeared in the isomerization process at various time intervals, were calculated from the data given in Table 3 and are shown in Figure 4 for the vesicular system. The accumulation of Cu^{II}-CA reaches a maximal value of 9% (based on the amount of $PL^{+}2C_{16}$ placed in the outer vesicle layer) after 30 s in the $N^{+}C_5Ala2C_{16}$ vesicle. On the other hand, as much as 22% was accumulated after 1 min in the CTAB micelle under the same conditions. The rate constants for protonation of Cu^{II}-CA (k_2 and k_3) in the vesicle are larger than the respective values in the micelle, while the rate constants for deprotonation of Cu^{II}-ASB (k_1) in both aggregate systems show the opposite correlation. Thus, the reaction site in the vesicle provides a more acidic microenvironment relative to that in the micelle at the same bulk pH. This is consistent with the findings that the K_{SB} value is smaller and the pK_a value of $PL^{+}2C_{16}$ is larger in the vesicle than the respective values in the micelle; pK_a values for the 3-hydroxy group of $PL^{+}2C_{16}$ are 3.5 and 3.1 in the $N^{+}C_5Ala2C_{16}$ vesicle and the CTAB micelle, respectively, at 30 °C as determined by spectrophotometric titration.

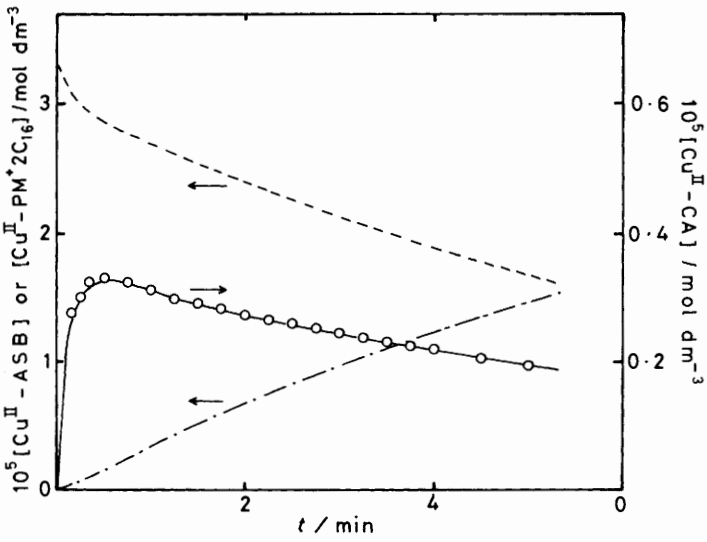

Figure 4. Distributions of Cu^{II}-CA (——), Cu^{II}-ASB (– – –), and $Cu^{II}\text{-PM}^{+}2C_{16}$ (— · — · —) at various time intervals for the transamination of L-Phe (4.5×10^{-3} mol dm^{-3}) with $PL^{+}2C_{16}$ (4.5×10^{-5} mol dm^{-3}) as catalysed by copper(II) ions (9.0×10^{-5} mol dm^{-3}) in the $N^{+}C_5Ala2C_{16}$ (1.0×10^{-3} mol dm^{-3}) vesicle; the copper(II) chelates being present in the outer vesicle layer. The curves drawn herein are calculated ones on the basis of kinetic parameters listed in Table 3, and the open circles denote experimentally observed values for Cu^{II}-CA

The collapse ratios of the Cu^{II}-CA species in terms of k_2/k_3 are 5.2 and 11 in the vesicular and micellar systems, respectively (A in Scheme 2). Thus, the transformation of Cu^{II}-CA into Cu^{II}-KSB is a kinetically unfavourable process in comparison with the competing formation of Cu^{II}-ASB from the same carbanion species. Cram and his co-workers have claimed that the collapse ratio for aza-allylic carbanions is controlled by electronic and steric effects originated from substituents.[20] For example, in the isomerization between *N*-(α-ethoxycarbonylneopentylidene)-α-(4-pyridyl)ethylamine and *N*-[α-(4-pyridyl)ethylidene]-α-ethoxycarbonylneopentylamine as catalysed by 1,5-diazabicyclo[4.3.0]non-5-ene in t-butyl alcohol, the carbanion intermediate was transformed into the latter more favourably than into the former[20b] (B in Scheme 2). In the light of Cram's concept, our present findings are consistent with the following explanation: the electronic effect by the carboxylate group prevails over steric hindrance by the benzyl group in the protonation of the copper(II)–carbanion chelate. In addition, the difference in the collapse ratio between the vesicular and micellar systems must come from differences in the microenvironmental properties around the two protonation sites. Since the pyridoxal moiety of $PL^{+}2C_{16}$ in the $N^{+}C_5Ala2C_{16}$ vesicle is tightly anchored in the hydrogen-belt domain where a slight displacement from one place to another is subjected to a significant change in the microenvironmental polarity,† the two protonation sites of Cu^{II}-CA must be placed in different circumstances. This environmental effect seems to differentiate the two aggregate systems in the collapse ratio. Apparently, the overall transamination reactivity is primarily controlled by the collapse ratio (Table 3).

* The calculation was also performed by taking ε as another unknown parameter, and the resulting ε value was identical with that evaluated experimentally. When the kinetic data were analysed on the basis of equation (7) with the assumption that $k_5 \gg k_3'$, we obtained $k_4 \cong 0$; the k_1, k_2, and k_3' values were identical with the k_1, k_2, and k_3 values, respectively, obtained from equation (4). This result is consistent with

$$Cu^{II}\text{-ASB} \underset{k_2}{\overset{k_1}{\rightleftharpoons}} Cu^{II}\text{-CA} \underset{k_4}{\overset{k_3'}{\rightleftharpoons}} Cu^{II}\text{-KSB} \xrightarrow{k_5} Cu^{II}\text{-PM}^{+}2C_{16} + KA \quad (7)$$

the observation that the hydrolysis of Cu^{II}-KSB is not involved in the rate-determining step along with the relation $k_5 \gg k_4$.

† The microscopic polarity in the centre of the hydrogen-belt domain, evaluated from the absorption maximum originated from the pyridoxal moiety of $PL^{+}2C_{16}$ [$E_T(30)$ 50.6], is lower than that in the outer vesicle domain, evaluated from the absorption maximum originated from the 1,4-dihydronicotinamide moiety [$E_T(30)$ 59].[21]

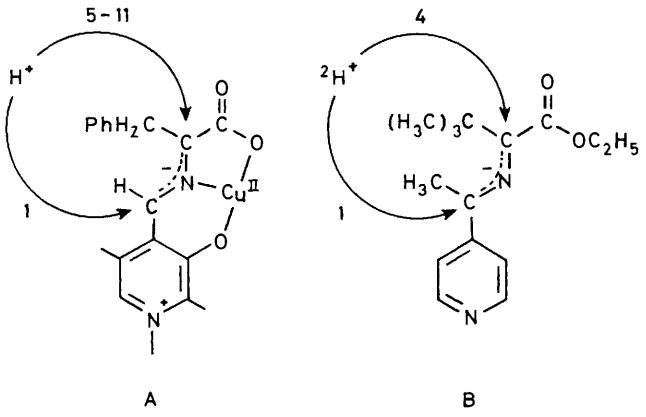

Scheme 2.

The formation of an aluminium(III) complex of an aldimine Schiff's base derived from pyridoxal and an α-amino acid was found to be more favourable than that of the corresponding ketimine chelate from the thermodynamic viewpoint. In addition, the isomerization between the two chelate species reaches an equilibrium involving primarily the aldimine species, regardlesss of the starting species: pyridoxal and ethyl alaninate or pyridoxamine and ethyl pyruvate,[17b] pyridoxal and alanine or pyridoxamine and pyruvic acid.[22] Thus, the isomerization of the aldimine Schiff's base to the corresponding ketimine is an unfavourable process not only thermodynamically but also kinetically. An acceleration of the hydrolysis of the ketimine Schiff's base chelate is inevitably important for the effective isomerization in the direction from the aldimine chelate to the ketimine. The present cationic molecular assemblies are valid for such catalysis.

In conclusion, the transamination of L-Phe, a hydrophobic α-amino acid, with PL^+2C_{16} was most effectively catalysed by copper(II) ions in the $N^+C_5Ala2C_{16}$ vesicle and the CTAB micelle. The catalytic activity of copper(II) ions is so large as to allow sufficient accumulation of the carbanion chelate as an intermediate in the aldimine–ketimine isomerization. The overall transamination reactivity is greater in the vesicle than in the micelle and primarily controlled by the collapse ratio. Even though the $N^+C_5His2C_{16}$ vesicle is far more effective than the molecular aggregates of $N^+C_5Ala2C_{16}$ and CTAB for rate enhancement of the present transamination as reported previously,[6a] application of the critical kinetic analysis to the former vesicular system was not possible due to incomplete formation of the aldimine Schiff's base in the initial stage of the reaction. Nevertheless, the kinetic conclusion obtained here is also applied plausibly to the reaction carried out in the $N^+C_5His2C_{16}$ vesicle.

Experimental

Materials.—L-Phenylalanine (Protein Research Foundation, Osaka, Japan), L-isoleucine, L-leucine, L-valine, L-alanine, L-glutamic acid (all from Wako Pure Chemical Industries, Osaka), 5,5-dithiobis-(2-nitrobenzoic acid), 1,6-diphenylhexa-1,3,5-triene (both from Nakarai Chemicals, Kyoto), 2,4-dinitrophenylhydrazine, sodium 2,4,6-trinitrobenzenesulphonate (both from Wako Pure Chemical Industries), and disodium ethylenediaminetetra-acetate (EDTA; Dojin Chemical Laboratories, Kumamoto) were obtained as guaranteed reagents and used without further purification. Hexadecyltrimethylammonium bromide (CTAB; Nakarai Chemicals) was recrystallized from ethanol, m.p. 237—239 °C (decomp.). Copper(II) perchlorate, zinc(II) perchlorate (both from Kishida Chemical Co., Osaka), iron(III) nitrate, and aluminium(III) nitrate (both from Wako Pure Chemical Industries) were dissolved in distilled and deionized water and standardized by conventional chelatometric titration. Preparation and characterization of *NN*-dihexadecyl-*N*$^{\alpha}$-[6-(trimethylammonio)hexanoyl]-L-alaninamide bromide ($N^+C_5Ala2C_{16}$),[3] 2-methyl-3-hydroxy-4-formyl-5-(dodecylthiomethyl)pyridine (PLC_{12}),[4a] and 1,2-dimethyl-3-hydroxy-4-formyl-5-hydroxymethylpyridinium chloride (PL^+C_1)[6b,23] have been reported elsewhere. 1-(*NN*-Dihexadecylcarbamoylmethyl)-2-methyl-3-hydroxy-4-formyl-5-hydroxymethylpyridinium chloride (PL^+2C_{16}) was prepared as described below.

NN-*Dihexadecyl-2-iodoacetoamide.*—Dicyclohexylcarbodiimide (2.6 g, 13 mmol) and dihexadecylamine (4.7 g, 10 mmol) were added in this sequence to a solution of iodoacetic acid (1.9 g, 10 mmol) in dry dichloromethane (30 ml) at 0 °C with stirring. The resulting mixture was stirred for 2 h at 0 °C and for a further 15 h at room temperature, and the precipitate (*NN*-dicyclohexylurea) was removed by filtration. The solvent was removed *in vacuo*, and the residue was dissolved in ethyl acetate (100 ml). The solution was then washed with 10% aqueous citric acid, 5% aqueous sodium hydrogencarbonate, and saturated aqueous sodium chloride in this sequence. After being dried over Na_2SO_4, the solution was evaporated *in vacuo* to give an oil. The crude product was purified by liquid chromatography on a column of silica gel (Wako Gel C-100) with chloroform as an eluant giving a pale yellow solid, yield 5.7 g (90%); R_F (silica gel f of Tokyo Kasei Kogyo Co., Tokyo; ethyl acetate) 0.89; m.p. 47.0—48.0 °C; δ_H (60 MHz; solvent $CDCl_3$; standard Me_4Si) 0.87 [6 H, t, $N(CH_2)_{15}CH_3$], 1.20 [56 H, m, $NCH_2(CH_2)_{14}CH_3$], 3.22 [4 H, t, $NCH_2(CH_2)_{14}CH_3$], and 3.69 (2 H, s, CH_2N).

1-(NN-*Dihexadecylcarbamoylmethyl*)-2-*methyl*-3-*hydroxy*-4,5-[*methanoxy*-(9-*methoxy*)*methano*]*pyridinium Chloride.*—A solution of pyridoxal monomethyl acetal[23] (500 mg, 3.0 mmol) and the above amide (1.9 g, 3.0 mmol) in benzene–methanol (10:1 v/v; 50 ml) was heated at 65 °C for 300 h in a sealed tube. The solvent was removed *in vacuo*, and the residue was purified by liquid chromatography on a column of silica gel (Wako Gel C-100) with ethanol as an eluant. The eluted product fraction was evaporated to dryness *in vacuo*, and the residue was dissolved in ethanol–water (1:1 v/v; 100 ml). Silver chloride (1.0 g, 7 mmol), prepared freshly from silver nitrate and potassium chloride, was added to the solution. The mixture was stirred for 4 h at room temperature, and then precipitates were removed by filtration. The filtrate was evaporated to dryness *in vacuo*, and the residue was purified by liquid chromatography on a column of silica gel (Wako Gel C-100) with ethanol as an eluant. Elimination of the solvent *in vacuo* gave a pale yellow solid, yield 30 mg (1.4%) (Found: C, 71.85; H, 10.9; N, 3.95. $C_{43}H_{79}ClN_2O_4$ requires C, 71.4; H, 11.0; N, 3.85%); R_F (silica gel f; ethyl acetate) 0.88; δ_H (60 MHz; solvent $CDCl_3$; standard Me_4Si) 0.88 [6 H, t, $N(CH_2)_{15}CH_3$], 1.26 [56 H, m, $NCH_2(CH_2)_{14}CH_3$], 2.32 (3 H, s, 2-CH_3 on pyridine ring), 3.25 [4 H, br t, $NCH_2(CH_2)_{14}CH_3$], 3.48 (3 H, s, CH_3O), 3.71 (2 H, s, 5-CH_2 on pyridine ring), 5.98 (2 H, s, CH_2CON), 6.19 (1 H, s, 4-CH on pyridine ring), and 6.88 (1 H, s, 6-H on pyridine ring).

1-(NN-*Dihexadecylcarbamoylmethyl*)-2-*methyl*-3-*hydroxy*-4-*formyl*-5-*hydroxymethylpyridinium Chloride* (PL^+2C_{16}).—Concentrated hydrochloric acid (10 ml; 12.1 mol dm^{-3}) was added to an ethanol solution (50 ml) of the above pyridinium chloride (15 mg, 0.021 mmol), and the mixture was stirred for 5 min at room temperature. After ethanol was removed *in vacuo*, the resulting aqueous mixture was extracted with dichloromethane. The extract was dried over Na_2SO_4 and evaporated

in vacuo to give a pale yellow solid (the hemiacetal form): yield 12 mg (80%) (Found: C, 69.2; H, 10.8; N, 3.75. $C_{42}H_{77}ClN_2O_4$ requires C, 69.35; H, 10.95; N, 3.85%); R_F (silica gel f, ethanol–chloroform 1:3 v/v) 0.87; $\nu_{max.}$ (KBr disk) 2 920 and 2 840 (CH) and 1 650 cm^{-1} (C=O), no aldehyde C=O; δ_H (60 MHz; solvent $CDCl_3$; standard Me_4Si) 0.88 [6 H, t, $N(CH_2)_{15}CH_3$], 1.23 [56 H, m, $NCH_2(CH_2)_{14}CH_3$], 2.52 (3 H, s, 2-CH_3 on pyridine ring), 3.31 [4 H, br t, $NCH_2(CH_2)_{14}CH_3$], 5.01 (2 H, s, 5-CH_2 on pyridine ring), 5.65 (2 H, s, CH_2CON), 6.57 (1 H, s, 4-CH on pyridine ring), and 7.96 (1 H, s, 6-H on pyridine ring).

General Measurements.—Elemental analyses were performed at the Microanalysis Centre of Kyushu University. A Beckman Φ71 pH meter equipped with a Beckman 39505 combined electrode was used for pH measurements after calibration with a combination of appropriate aqueous standard buffers. ^1H N.m.r. spectra were taken on a Hitachi R-24B spectrometer. Electronic absorption spectra were obtained with a Hitachi 220A or a Union Giken SM-401 high sensitivity spectrophotometer. I.r. spectra were recorded on a JASCO IR-810 spectrophotometer. Fluorescence polarization measurements were carried out on a Union Giken FS-501A spectrophotometer equipped with a Sord M200 Mark II microcomputer. The steady-state fluorescence anisotropy (r_s) was calculated by equation (8), where I is the fluorescence intensity, and the

$$r_s = (I_{vv} - C_f I_{vh})/(I_{vv} + 2C_f I_{vh}) \quad (8)$$

subscripts v and h refer to the orientations, vertical and horizontal, respectively, for the excitation and analyser polarizers in this sequence. C_f is the grating correction factor, given by I_{hv}/I_{hh}. The r_s value is alternatively given by equation (9), where τ is the fluorescence lifetime of a probe, ρ is the

$$1/r_s = (1/r_{s.0})(1 + 3\tau/\rho) \quad (9)$$

relaxation time for rotation of a probe, and $r_{s.0}$ refers to the maximal value of r_s in the absence of any rotational motion of a probe.[24] Negatively stained electron micrographs were taken on a JEOL JEM-2000FX electron microscope in a manner as described previously.[3]

Kinetic Measurements.—A solution of the single-walled co-vesicle composed of $N^+C_5Ala2C_{16}$ (*ca.* 1×10^{-3} mol dm^{-3}) and PL^+2C_{16} (*ca.* 5×10^{-5} mol dm^{-3}) in an aqueous carbonate buffer (0.02 mol dm^{-3}) at μ 0.10 (KCl) was prepared in a manner similar to that reported elsewhere.[6b] After addition of L-phenylalanine (*ca.* 5×10^{-3} mol dm^{-3}) dissolved in the aqueous carbonate buffer (200 μl) to the vesicle solution (2 ml), formation of the aldimine Schiff's base reached an equilibrium within 30 min. At this stage, each kinetic run was initiated by adding an appropriate amount (0—20 μl) of an aqueous solution of metal ions to the equilibrated solution. Progress of the reaction was followed by means of electronic absorption spectroscopy. The rapid metal chelate formation from the aldimine Schiff's base and copper(II) ions were monitored with a Union Giken RA-401 stopped-flow spectrophotometer.

Product Analyses.—The remaining PL^+2C_{16} in the $N^+C_5Ala2C_{16}$ vesicle with or without copper(II) ions was separated from the reaction mixture and converted into the corresponding 2,4-dinitrophenylhydrazone as follows. The mixture (2.2 ml) was extracted with chloroform (50 ml) after the kinetic measurement, and the organic layer was washed sequentially with 1 mol dm^{-3} aqueous hydrochloric acid (15 ml × 3), 5% aqueous sodium hydrogencarbonate (15 ml × 3), and saturated aqueous sodium chloride (10 ml × 1). After being dried over Na_2SO_4, the chloroform extract was evaporated to dryness *in vacuo*. Aqueous CTAB (500 μl; 3 mmol dm^{-3}) and aqueous hydrochloric acid (100 μl; 2 mol dm^{-3}) containing 2,4-dinitrophenylhydrazine (5 mmol dm^{-3}) were added to the residue in this sequence, and the mixture was allowed to stand for 5 min at room temperature. Aqueous phosphate buffer (700 μl; 0.2 mol dm^{-3}) containing sodium hydroxide (0.4 mol dm^{-3}) was added to the mixture to attain pH 7.0. Upon addition of aqueous sodium hydroxide (1 ml; 2.5 mol dm^{-3}) to the mixture, the absorption intensity originated from the 2,4-dinitrophenylhydrazone of PL^+2C_{16} was measured at 530 nm. β-Phenylpyruvate produced by the transamination remained in the aqueous layer during the extraction treatment. The amount of the keto acid was also evaluated by converting it into the corresponding 2,4-dinitrophenylhydrazone in a similar manner.

The hydrophobic pyridoxamine (PM^+2C_{16}) derived from PL^+2C_{16} during transamination was extracted with chloroform from the reaction mixture and separated by gel filtration chromatography on a column of Sephadex LH-20 with methanol as an eluant. The fraction having an absorption at 335 nm was collected and evaporated to dryness *in vacuo*. After addition of water (2 ml) to the residue, the mixture was sonicated at 30 W for 1 min with a bath-type sonicator (Bransonic 12, Yamato Scientific Co., Tokyo). Then, aqueous potassium carbonate (2 ml; 1 mol dm^{-3}), aqueous sodium 2,4,6-trinitrobenzenesulphonate (TNBS; 2 ml; 10 mmol dm^{-3}), and toluene (4 ml) were added sequentially to the solution, and vortex mixing was applied for 20 s to the resulting mixture. After separation of the aqueous layer, the adduct of TNBS with PM^+2C_{16}, dissolved in the organic layer, was subjected to quantitative analysis by spectrophotometric means with attention to absorption maxima at 358 and 420 nm.[25] The adduct of TNBS with L-phenylalanine was not extracted into the organic layer under the present conditions.

Acknowledgements

This work was supported in part by a Grant-in-Aid for Scientific Research from the Ministry of Education, Science, and Culture of Japan.

References

1 E. E. Snell and S. J. Di Mari, in 'The Enzymes,' ed. P. D. Boyer, Academic Press, New York, 1970, 3rd edn., vol. 2, pp. 335—370.
2 (*a*) T. C. Bruice and S. J. Benkovic, 'Bioorganic Mechanisms,' Benjamin, New York, 1966, vol. 2, pp. 226—300; (*b*) A. E. Martell, in 'Advances in Enzymology,' ed. A. Meister, Wiley, New York, 1982, vol. 53, pp. 163—199.
3 Y. Murakami, A. Nakano, A. Yoshimatsu, K. Uchitomi, and Y. Matsuda, *J. Am. Chem. Soc.*, 1984, **106**, 3613.
4 (*a*) Y. Murakami, J. Kikuchi, A. Nakano, K. Akiyoshi, and T. Imori, *Bull. Chem. Soc. Jpn.*, 1984, **57**, 1116; (*b*) Y. Murakami, J. Kikuchi, and K. Akiyoshi, *Chem. Lett.*, 1984, 1185; (*c*) Y. Murakami, J. Kikuchi, and K. Akiyoshi, *Bull. Chem. Soc. Jpn.*, 1985, **58**, 1200.
5 Y. Murakami, A. Nakano, and K. Akiyoshi, *Bull. Chem. Soc. Jpn.*, 1982, **55**, 3004.
6 (*a*) Y. Murakami, J. Kikuchi, T. Imori, and K. Akiyoshi, *J. Chem. Soc., Chem. Commun.*, 1984, 1434; (*b*) Y. Murakami, J. Kikuchi, K. Akiyoshi, and T. Imori, *J. Chem. Soc., Perkin Trans. 2*, 1985, 1919.
7 (*a*) Y. Murakami and H. Kondo, *Bull. Chem. Soc. Jpn.*, 1975, **48**, 541; (*b*) H. Kondo, J. Kikuchi, and J. Sunamoto, *Tetrahedron Lett.*, 1983, **24**, 2403; (*c*) H. Kondo, J. Kikuchi, S. Uchida, T. Kitamikado, E. Koyanagi, and J. Sunamoto, *Bull. Chem. Soc. Jpn.*, 1985, **58**, 675.
8 Y. N. Belokon', V. I. Tararov, T. F. Savel'eva, and V. M. Belikov, *Makromol. Chem.*, 1980, **181**, 2183.
9 (*a*) H. Kuzuhara, M. Iwata, and S. Emoto, *J. Am. Chem. Soc.*, 1977, **99**, 4173; (*b*) J. Winkler, E. Coutouli-Argyropoulou, R. Leppkes, and R. Breslow, *ibid.*, 1983, **105**, 7198.
10 R. Breslow, M. Hammond, and M. Lauer, *J. Am. Chem. Soc.*, 1980, **102**, 421.

11 (*a*) J. B. Longenecker and E. E. Snell, *J. Am. Chem. Soc.*, 1957, **79**, 142; (*b*) Y. Matsushima and A. E. Martell, *ibid.*, 1967, **89**, 1331; (*c*) O. A. Gansow and R. H. Holm, *ibid.*, 1969, **91**, 5984.
12 T. C. Bruice and R. M. Topping, *J. Am. Chem. Soc.*, (*a*) 1963, **85**, 1480; (*b*) p. 1488; (*c*) p. 1493; (*d*) J. W. Thanassi, A. R. Butler, and T. C. Bruice, *Biochemistry*, 1965, **4**, 1463; D. S. Auld and T. C. Bruice, *J. Am. Chem. Soc.*, (*e*) 1967, **89**, 2090; (*f*) p. 2098.
13 J. R. Maley and T. C. Bruice, (*a*) *J. Am. Chem. Soc.*, 1968, **90**, 2843; (*b*) *Arch. Biochem. Biophys.*, 1970, **136**, 187.
14 H. A. Benesi and J. H. Hildebrand, *J. Am. Chem. Soc.*, 1949, **71**, 2703.
15 (*a*) W. T. Jenkins, *J. Biol. Chem.*, 1964, **239**, 1742; (*b*) F. S. Furbish, M. L. Fonda, and D. E. Metzler, *Biochemistry*, 1969, **8**, 5169; (*c*) M. Martinez-Carrion, D. C. Tiemeier, and D. L. Peterson, *ibid.*, 1970, **9**, 2574.
16 L. Schirch and R. A. Slotter, *Biochemistry*, 1966, **5**, 3175.
17 S. Matsumoto and Y. Matsushima, *J. Am. Chem. Soc.*, (*a*) 1972, **94**, 7211; (*b*) 1974, **96**, 5228.
18 J. H. Fendler and W. L. Hinze, *J. Am. Chem. Soc.*, 1981, **103**, 5439.
19 A. A. Frost and R. G. Pearson, 'Kinetics and Mechanism,' Wiley, New York, 1961, 2nd edn., pp. 173—177.
20 (*a*) D. A. Jaeger and D. J. Cram, *J. Am. Chem. Soc.*, 1971, **93**, 5153; (*b*) D. A. Jaeger, M. D. Broadhurst, and D. J. Cram. *ibid.*, 1979, **101**, 717.
21 (*a*) Y. Murakami, J. Kikuchi, K. Nishida, and A. Nakano, *Bull. Chem. Soc. Jpn.*, 1984, **57**, 1371; (*b*) E. M. Kosower, 'An Introduction to Physical Organic Chemistry,' Wiley, New York, 1968, pp. 293—316.
22 A. E. Martell and P. Taylor, *Inorg. Chem.*, 1984, **23**, 2734.
23 D. Heyl, E. Luz, S. A. Harris, and K. Folkers, *J. Am. Chem. Soc.*, 1951, **73**, 3430.
24 G. Weber, *Adv. Protein Chem.*, 1953, **8**, 415.
25 A. P. H. Phan, T. T. Ngo, and H. M. Lenhoff, *Appl. Biochem. Biotech.*, 1983, **8**, 127.

Received 15*th October* 1985; *Paper* 5/1783